



Direct Laser Writing of Computer-Generated Holograms by Photodissolution of Silver in Arsenic Trisulfide

Arjun Karimbana Kandy, Cedric Sebastien Martins Figueiredo, Manuel Fernandez Merino, Antoine Bourgade, Jean-Yves Natoli, Konstantinos Iliopoulos, Julien Lumeau

► To cite this version:

Arjun Karimbana Kandy, Cedric Sebastien Martins Figueiredo, Manuel Fernandez Merino, Antoine Bourgade, Jean-Yves Natoli, et al.. Direct Laser Writing of Computer-Generated Holograms by Photodissolution of Silver in Arsenic Trisulfide. *Optics*, 2023, 4 (1), pp.138 - 145. 10.3390/opt4010010 . hal-04265706

HAL Id: hal-04265706

<https://hal.science/hal-04265706v1>

Submitted on 31 Oct 2023

HAL is a multi-disciplinary open access archive for the deposit and dissemination of scientific research documents, whether they are published or not. The documents may come from teaching and research institutions in France or abroad, or from public or private research centers.

L'archive ouverte pluridisciplinaire **HAL**, est destinée au dépôt et à la diffusion de documents scientifiques de niveau recherche, publiés ou non, émanant des établissements d'enseignement et de recherche français ou étrangers, des laboratoires publics ou privés.

Article

Direct Laser Writing of Computer-Generated Holograms by Photodissolution of Silver in Arsenic Trisulfide

Arjun Karimbana Kandy , Cedric Sébastien Martins Figueiredo, Manuel Fernandez Merino , Antoine Bourgade, Jean-Yves Natoli, Konstantinos Iliopoulos and Julien Lumeau  *

Aix Marseille Univ, CNRS, Centrale Marseille, Institut Fresnel, Marseille, France

* Correspondence: julien.lumeau@fresnel.fr

Abstract: Photodissolution is a process that is well known for its ability to cause inclusion of silver into the matrix of a chalcogenide layer, changing its optical properties. In this paper, using e-beam deposition, we developed Ag (74 nm)/As₂S₃ (355 nm) bilayers and characterized the photodissolution kinetics when exposed to actinic radiation. We showed that local complete silver photodissolution at the micron scale can be achieved. Based on this result, we then developed amplitude-based computer-generated holograms using direct laser writing. CW lasers with beam shaping and short pulse lasers with beam scanning were both implemented. Elements with 8.5 μm and <1 μm spatial resolution and close to theoretical intensity distribution, respectively, were successfully demonstrated.

Keywords: chalcogenides; photodissolution; computer-generated holograms; e-beam deposition



Citation: Karimbana Kandy, A.; Figueiredo, C.S.M.; Fernandez Merino, M.; Bourgade, A.; Natoli, J.-Y.; Iliopoulos, K.; Lumeau, J. Direct Laser Writing of Computer-Generated Holograms by Photodissolution of Silver in Arsenic Trisulfide. *Optics* **2023**, *4*, 138–145. <https://doi.org/10.3390/opt4010010>

Academic Editor: David A. Willis

Received: 18 November 2022

Revised: 18 January 2023

Accepted: 28 January 2023

Published: 31 January 2023

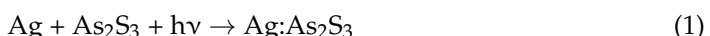


Copyright: © 2023 by the authors. Licensee MDPI, Basel, Switzerland. This article is an open access article distributed under the terms and conditions of the Creative Commons Attribution (CC BY) license (<https://creativecommons.org/licenses/by/4.0/>).

1. Introduction

The emergence of new technologies and the wide range of applications for lasers require new components to modify laser properties such as their intensity profile. Laser printing systems, optical data storage, and optical trapping are a few examples in which beam shaping techniques have important roles [1]. Computer-generated holograms (CGHs) and diffractive optical elements (DOEs) enable an effective and easy way to modify the typical Gaussian intensity profile of a laser beam. The traditional fabrication methods of CGHs or DOEs rely on photolithographic processes that require several steps and can be time-consuming. In recent works, it has been shown that basic diffractive optical elements could be recorded in chalcogenide layers based on photo-induced refractive index change [2,3]. However, due to limited refractive index change, thick layers, up to 15–25 μm, were required to generate the desired phase change. An alternative approach to generating DOEs is by changing the locally transmitted amplitude instead of the locally transmitted phase. However, the amplitude CGHs for beam shaping are achievable by using the same patterns as those used to produce phase elements [4].

In this work, we investigated the use of silver photodissolution to produce a flat amplitude CGH with a single step fabrication. Photodissolution is a phenomenon where a photochemical reaction causes the integration of a metal layer in an underlying amorphous chalcogenide layer, following a reaction also known as photodoping:



Even though it had been observed before, the research on this topic really started in 1971, when it was first proposed as a photo-microfabrication method [5]. Several combinations of metals and chalcogenides have been proven to give rise to photodissolution, with efficiencies and effects depending on the involved materials. However, it has been shown that Ag yields the highest rates of photodissolution [6]. Different possibilities of metal chalcogenide have been studied and their ability to produce photodissolution has

been quantified [7]. However, the most efficient one, to date, appears to be the combination of Ag and As₂S₃, which was chosen for this study.

While such effects have thoroughly been studied in the past, there have been no, or few, applications of this effect for the fabrication of optical elements and, in most of the literature, this effect has been introduced as an efficient method for enhancing photoinduced refractive index change. However, silver photodissolution in the As₂S₃ layer appears to be a very promising way to fabricate amplitude elements such as CGHs that work over a broad spectral range. No lithographic process is needed, and microstructures can directly be recorded, using laser light, into the SiO₂/As₂S₃/Ag/glass stack resulting in a plane parallel element.

In this paper, first, we investigated the fabrication process of such a stack, and then the associated photodissolution kinetics. Such a preliminary study is necessary as the process is highly dependent on the fabrication procedure. Then, we investigated two alternative methods for recording of amplitude CGH. The first method relies on a CW laser, in which spatial intensity distribution is shaped with a LCD display, and then imaged in the recording plane where the SiO₂/As₂S₃/Ag/glass stack is placed. The second method improves the spatial resolution with the use of a femtosecond laser focused in the sample plane and scanned across its aperture. Comparison between both techniques is finally provided.

2. Materials and Methods

2.1. Thin Film Deposition

Bilayer structures composed of films of As₂S₃/Ag on 25 mm diameter B270 glass substrates were prepared. The samples were manufactured by physical vapor deposition in a vacuum of 10⁻⁶ mbar using a Bühler/Leybold Optics SYRUSpro 710 plasma-assisted e-beam deposition machine. Each film thickness was monitored through a quartz-crystal microbalance which was also used to measure the deposition rates. The rates were maintained constant during the deposition and set to 0.7 nm/s for the As₂S₃ layer, and 0.5 nm/s for the Ag one. To protect the system, an additional thin capping layer of SiO₂ was deposited on top at a 0.5 nm/s rate. The result was a SiO₂/As₂S₃/Ag/glass stack with respective thicknesses of 10 nm, 355 nm, and 74 nm.

2.2. Kinetics of the Photodissolution

We studied the kinetics of the photodissolution when exposed to a blue LED emitting at 470 nm and with typically 200 μW/cm² power density. With such a source having a wavelength close to the chalcogenide bandgap, high absorption is achieved and photodissolution of silver in As₂S₃ can be triggered. The transmission spectrum of the stack was first measured, before exposure and after complete exposure, using a Perkin Elmer Lambda 1050 in the 450–850 nm spectral range (Figure 1).

The initial transmission of the sample is below 2% with oscillations related to the interference effects that occur within the As₂S₃ layer. Reverse engineering using thin-film dedicated software (Optilayer [8]) based on matrix formalism [9] confirmed that the thickness of each layer was equal to the one that was specified during the fabrication. The discrepancy that can be seen between the experimental curves and the model can easily be explained by the fact that the Ag dispersion model we used was taken from the literature [10]. However, it is well known that the dispersion model of thin-film materials depends on the fabrication procedure as well as their surrounding materials (especially Ag). As the goal of this analysis was to qualitatively analyze the photodissolution kinetics, we decided not to refine the model. The transmission after exposure reached 92% at 800 nm, confirming that all Ag has been dissolved into the As₂S₃ layer. A similar reverse engineering approach allowed us to determine the new parameters of the stack after exposure. The As₂S₃/Ag stack became a single Ag:As₂S₃ layer with a refractive index ~0.5 higher than the refractive index of the undoped As₂S₃ layer (going from 2.5 to 3) and with a thickness of 428 ± 3 nm. This result meant that the thickness of the Ag:As₂S₃ layer was identical to

that of the $\text{As}_2\text{S}_3/\text{Ag}$ stack. Optical profilometer measurement at the boundary between unexposed and exposed regions confirmed that there was no change in the overall stack thickness, but photodissolution resulted in a parasitic increase of the roughness from 0.5 nm RMS to 6 nm RMS.

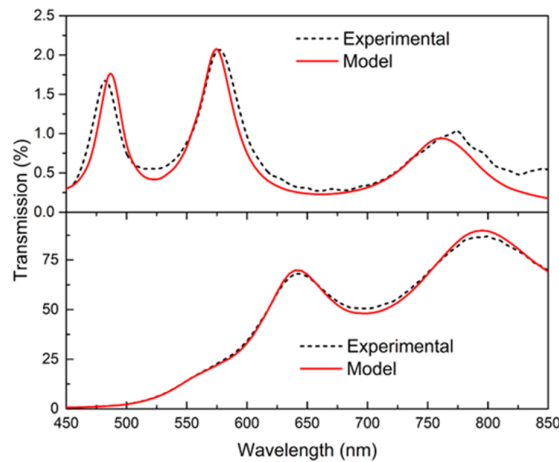


Figure 1. Spectral dependence of the transmission of the fabricated samples. Top graph, spectrum before exposure and bottom graph, spectrum after exposure. The experimental spectra are in black, and the spectra that were modeled using thin film models are in red.

2.3. Fabrication of Diffractive Optical Element (DOE) Using a CW laser

In this work, to record amplitude CGHs, two dedicated optical setups were especially developed for the controlled exposure of the samples. A continuous-wave laser and a femtosecond pulsed laser were employed. Concerning the former setup (Figure 2), a green TEM_{00} 532 nm continuous-wave laser with a power of 250 mW was employed for the photodissolution of Ag in As_2S_3 . First, a beam expander was used to create a 10 mm diameter collimated beam that was transmitted through a liquid crystal spatial light modulator (SLM). The SLM, placed in between crossed polarizers, was used to produce an amplitude profile with a pixel size of 8.5 μm . Then, the amplitude pattern generated on the SLM was imaged using a two-lens system with $1\times$ magnification directly on the thin-film stack surface in order to produce an identical amplitude pattern in the sample through photodissolution. Binary CGH has been fabricated using this method.

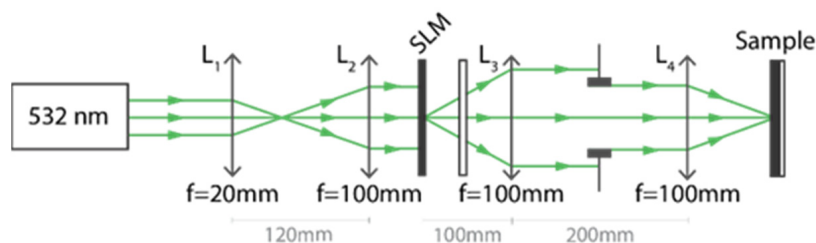


Figure 2. Optical setup for the direct writing of CGHs through photodissolution. The 532 nm continuous-wave laser is expanded with $5\times$ magnification using two achromatic lenses, L_1 and L_2 , and shines a spatial light modulator (SLM). L_3 and L_4 are two additional achromatic lenses that image the SLM on the sample plane with a $1\times$ magnification.

2.4. Fabrication of Diffractive Optical Element (DOE) Using a Femtosecond Laser

A passively mode-locked femtosecond laser that delivered 400 femtosecond pulses at 1030 nm fundamental wavelength with an adjustable repetition rate was employed for direct CGH writing (Figure 3). A second harmonic crystal (BBO) was used for frequency doubling. Then, the frequency-doubled femtosecond laser beam ($\lambda = 515 \text{ nm}$) was focused on the sample with a $50\times$ magnification microscope objective lens with a 0.5 numerical

aperture. The sample was exposed to the laser for an interval of 1 ms per pixel at an operating repetition rate of 200 kHz. The sample was mounted on a high-precision XYZ translational stage. The translational stage and the laser were coupled and controlled through a purpose-made LabVIEW program. Digital binary CGHs spatial patterns were fed to the LabVIEW program, which then precisely moved the sample and irradiated it with the laser accordingly to fabricate the patterns.

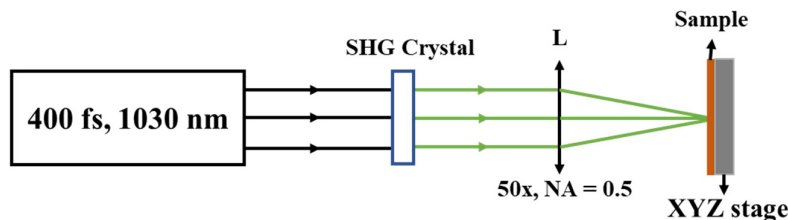


Figure 3. Optical setup for the direct femtosecond laser writing of CGHs through photodissolution.

3. Results

The kinetics of the photodissolution were studied with increasing dosage up to approximately 0.3 J/cm^2 (Figure 4a,b). Increasing the dosage of exposure results in a gradual increase in the sample transparency. At the first stage of the exposure, the transmission increase is very slow. This can be easily explained by the exponential dependence of the transmission on Ag thickness. Indeed, a simple calculation allows us to show that if a photodissolution of half of the Ag has occurred, i.e., if the thickness of Ag decreases from 74 to 37 nm, the sample average transmission will increase from 1 to 7%. Such an effect can be observed during the first quarter of the exposure for dosage up to 0.07 J/cm^2 . Other effects can be seen such as a red shift of the spectrum [11]. This effect reveals an increase in the optical thickness of the transparent layer related to both an increase in the refractive index and a real increase in the physical thickness of the transparent layer (from 355 to 428 nm). Increasing the dosage of exposure results in a complete photodissolution of silver after 0.15 J/cm^2 , the peak at 800 nm being the maximum. However, processes appear to be non-complete as an absorption band between 600 nm and 650 nm remains and tends to disappear as exposure is increased up to 0.3 J/cm^2 . This absorption is most likely due to plasmon resonance of the silver particles that dissolved in the As_2S_3 layer and that are then bleached during a second process requiring larger exposure dosages [12,13]. Additional information on the kinetics of the photodissolution can be found in [14].

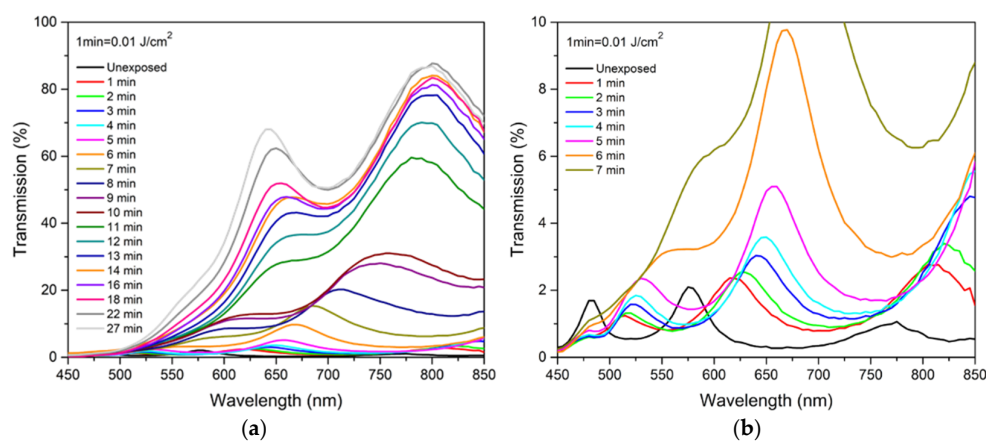


Figure 4. (a) Evolution of the spectral dependence of the transmission of the $\text{As}_2\text{S}_3/\text{Ag}$ structure for different dosages of exposure at 470 nm—overall process. (b) Evolution of the spectral dependence of the transmission of the $\text{As}_2\text{S}_3/\text{Ag}$ structure for different dosages of exposure at 470 nm—highlights the early-stage mechanisms.

Two different CGHs with different pitch sizes were then recorded using the experimental setups given in Figures 2 and 3. The amplitude profiles to be recorded were calculated using the VirtualLab Fusion software and designed to be compatible with the $8.5\text{ }\mu\text{m}$ resolution of the SLM. With such a large pitch, only limited diffraction angles were achieved, and the calculated far field profiles exhibited noise, especially for the largest patterns. Nevertheless, the potential of this method to record microstructures with different sizes was verified, especially when sub-micron resolution was achieved with femtosecond laser exposure. The exposure time for all the CGHs profiles using CW laser was set to ~ 4 min. Indeed, such exposure enabled the complete photodissolution of Ag in As_2S_3 . The first element generates a crosshair target visor with the feature's sizes going from 20 to $500\text{ }\mu\text{m}$, while the second element results in two symmetrical guitars and has a typical pitch of $50\text{ }\mu\text{m}$. In the case of femtosecond laser exposure, the patterns being the same, the typical pitches are one order of magnitude smaller.

First, these two types of elements were recorded using the setup shown in Figure 2, and then the diffraction patterns were characterized using a 633 nm He-Ne laser using a CCD camera in the focal plane of a 100 mm focal length lens. The recorded amplitude profile was also characterized using an optical microscope and compared to the theoretical profiles. Figure 5 shows a comparison between the theoretical and experimental amplitude profiles recorded in the multilayer stack. Figure 6 shows a comparison between the theoretical and experimental far-field diffracted intensity profiles for each type of CGH. Similar images were observed when characterized with lasers at longer wavelengths (e.g., 808 nm).

It has been shown in the past that efficient photodissolution can be also achieved by using pulsed lasers [15]. A similar technique has been utilized in this work to achieve photodissolution. In order to enhance the spatial resolution during the recording, a femtosecond direct laser writing setup was employed (Figure 3). The combination of well adjusted, high repetition rate, and laser fluence can induce photodissolution. The $\text{Ag:As}_2\text{S}_3$ was exposed at different combinations of repetition rates and energy per pulse to achieve large-area direct laser writing within minimal writing time. The laser irradiation parameters were optimized and set to an operating repetition rate of 200 kHz , 1 ms exposure time, and laser fluence between $0.01\text{--}0.03\text{ J/cm}^2$, to achieve good quality diffracted images. The applied fluence is well below the damage threshold of silver thin films as reported previously, which is between $0.25\text{--}3\text{ J/cm}^2$ [16,17].

The smallest feature size of the binary CGHs recorded using this setup was about $1\text{ }\mu\text{m}$, i.e., one order of magnitude smaller as compared with the previous setup. The feature size is limited to $1\text{ }\mu\text{m}$, due to the diffraction limit associated with the focusing objective lens, as well as the thermal propagation that arises during laser irradiation.

Figure 7 represents the microscopy image of the amplitude diffraction pattern recorded using femtosecond laser pulses (left) and the far-field diffracted image captured by transmitting a He-Ne laser through the recorded pattern (right).

All the recorded amplitude profiles, using both of the experimental setups, are very close to the theoretical ones, even for the smallest pitch size. For example, all features of the crosshair target visor amplitude profiles were accurately reproduced, even the small dots in the middle of the uniform zones. Similarly, the amplitude profiles of the guitars were well reproduced with sharp transitions between dark and clear regions. Regarding the intensity profiles, there is also a good agreement between the theoretical and experimental profiles. Sharp and quickly diverging diffracting images were achieved in the case of the femtosecond direct laser writing. Finally, zero order can be seen in both writing cases, however, the intensity of these zero orders does not exceed a few percent of the total intensity in the measurement plane. However, one must notice that the scale bars for amplitude profiles are one order of magnitude smaller in the case of femtosecond laser writing as compared with the CW laser writing. Therefore, this confirms the ability to record close to diffraction limit patterns with this method. A smaller resolution could be obtained with CW laser writing if a different imaging system was used to image the LCD

in the recording plane. However, to obtain a resolution below 1 μm would require a more complex optical scheme.

Finally, while the recording time is longer with femtosecond laser writing as compared with CW laser writing since it requires scanning the sample, it is more versatile. Indeed, as the recorded pitch size was considerably smaller than the previous CGHs (about one order of magnitude), larger diffraction angles were achieved for femtosecond laser generated elements, resulting in a sharp and quickly diverging diffracted image. The diffracted images obtained with the femtosecond laser contained more details as compared with those obtained with continuous laser writing (Figure 6 (right) and Figure 7 (right)).

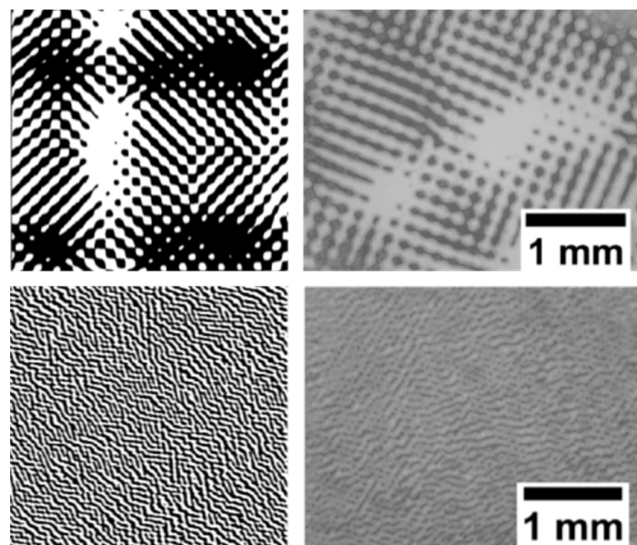


Figure 5. Comparison between the theoretical (left) and experimental (right) amplitude profiles recorded in the multilayer stack. Top, crosshair target visor and bottom, guitars.

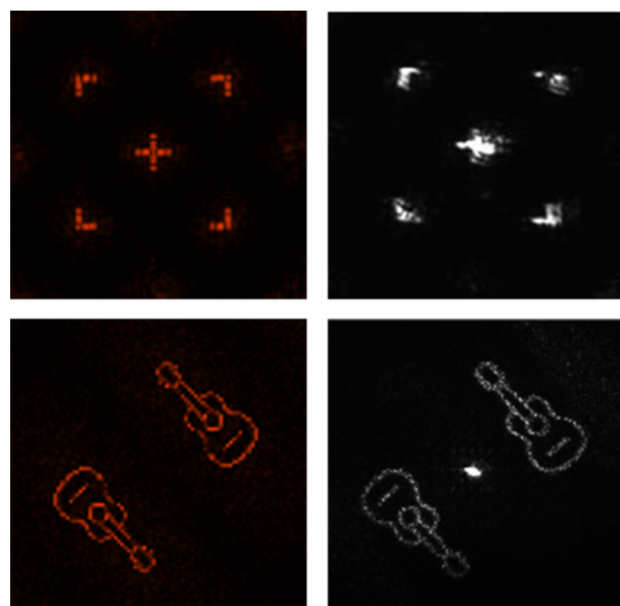


Figure 6. Comparison between the theoretical (left) and experimental (right) far-field diffracted intensity profiles of the CGHs. Top, crosshair target visor and bottom, guitars.

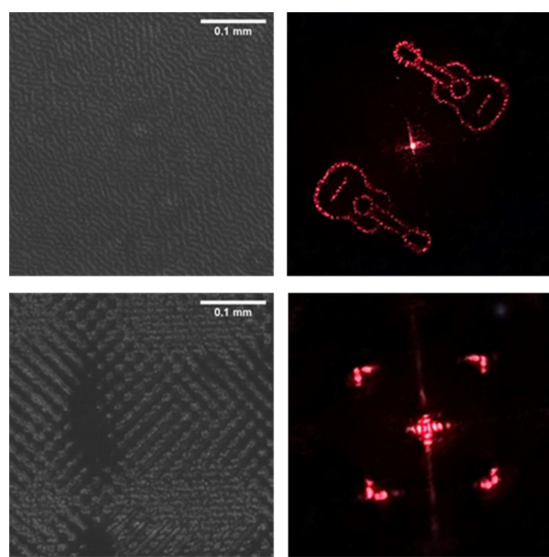


Figure 7. Recorded amplitude profiles (**left**) using the femtosecond laser and corresponding diffracted far field image (**right**).

4. Conclusions

In this work, an alternative method for the fabrication of computer-generated holograms was proposed and successfully proved. Instead of traditional photolithography, a direct laser writing procedure was employed. Continuous-wave and femtosecond lasers were employed to locally photodissolve a thin layer of silver (74 nm) in a matrix of As₂S₃ (354 nm), reproducing an amplitude pattern that works as a computer-generated hologram for beam shaping. First, the photodissolution kinetics were characterized. Then, elements with 8.5 μm and <1 μm spatial resolution and close to theoretical performances, respectively, were demonstrated. The produced elements remain flat thanks to the dissolution process, and therefore, are less sensitive to the environment (if they are protected from short wavelength radiations). In addition, due to the broad spectral performances of both Ag and As₂S₃, Ag + As₂S₃ beam shaping could be achieved up to 10+ μm if the layers were deposited on visible and infrared transparent substrates such as, for example, ZnSe.

Author Contributions: Conceptualization, K.I., J.-Y.N. and J.L.; methodology, A.K.K., C.S.M.F., M.F.M. and A.B.; investigation, A.K.K., C.S.M.F., M.F.M. and A.B.; writing—original draft preparation, A.K.K., C.S.M.F., M.F.M. and A.B.; writing—review and editing, K.I., J.-Y.N. and J.L.; visualization, A.K.K., C.S.M.F., M.F.M. and A.B.; supervision, K.I., J.-Y.N. and J.L.; project administration, K.I., J.-Y.N. and J.L.; funding acquisition, K.I., J.-Y.N. and J.L. All authors have read and agreed to the published version of the manuscript.

Funding: This research was funded by the French National Research Agency, grant number (ANR-19-CE09-0002-01), from the Ministry for Armed Forces (DGA), and Aix-Marseille University.

Data Availability Statement: The datasets generated during and/or analysed during the current study are available from the corresponding author on reasonable request.

Acknowledgments: The authors want to thank Charles Moisset of Institut Fresnel for the help with AFM measurements and Kevin Heggarty from Telecom Bretagne for providing access and guidance for the design of CGH.

Conflicts of Interest: The authors declare no conflict of interest.

References

1. Voelkel, R. Micro-Optics for Illumination Light Shaping in Photolithography. In *Laser Beam Shaping Applications*; CRC Press: Boca Raton, FL, USA, 2016; ISBN 978-1-315-37130-6.
2. Joerg, A.; Lumeau, J. Fabrication of Binary Volumetric Diffractive Optical Elements in Photosensitive Chalcogenide AMTIR-1 Layers. *Opt. Lett.* **2015**, *40*, 3233–3236. [CrossRef] [PubMed]

3. Joerg, A.; Vigneaux, M.; Lumeau, J. Versatile Digital Micromirror Device-Based Method for the Recording of Multilevel Optical Diffractive Elements in Photosensitive Chalcogenide Layers (AMTIR-1). *Opt. Lett.* **2016**, *41*, 3415–3418. [[CrossRef](#)] [[PubMed](#)]
4. Lohmann, A.W.; Paris, D.P. Binary Fraunhofer Holograms, Generated by Computer. *Appl. Opt. AO* **1967**, *6*, 1739–1748. [[CrossRef](#)] [[PubMed](#)]
5. Shimizu, I.; Sakuma, H.; Kokado, H.; Inoue, E. The Photo-Doping of Metals into Solids for New-Type Imaging Systems. *BCSJ* **1971**, *44*, 1173. [[CrossRef](#)]
6. Modifications Induced in Non-Crystalline Chalcogenides. In *Non-Crystalline Chalcogenides*; Popescu, M.A. (Ed.) Solid-State Science and Technology Library; Springer: Dordrecht, The Netherlands, 2000; pp. 209–292. ISBN 978-0-306-47129-2.
7. Tanaka, K.; Shimakawa, K. Chalcogenide Glasses in Japan: A Review on Photoinduced Phenomena. *Phys. Status Solidi B* **2009**, *246*, 1744–1757. [[CrossRef](#)]
8. Available online: <https://www.optilayer.com> (accessed on 30 January 2023).
9. Macleod, H.A. *Thin-Film Optical Filters*, 4th ed.; CRC Press/Taylor & Francis: Boca Raton, FL, USA, 2010.
10. Palik, E.D. *Handbook of Optical Constants and Solids*; Academic: Orlando, FL, USA, 1985.
11. Frumar, M.; Wagner, T. Ag Doped Chalcogenide Glasses and Their Applications. *Curr. Opin. Solid State Mater. Sci.* **2003**, *7*, 117–126. [[CrossRef](#)]
12. Gupta, R.; Dyer, M.J.; Weimer, W.A. Preparation and Characterization of Surface Plasmon Resonance Tunable Gold and Silver Films. *J. Appl. Phys.* **2002**, *92*, 5264–5271. [[CrossRef](#)]
13. Weimer, W.A.; Dyer, M.J. Tunable Surface Plasmon Resonance Silver Films. *Appl. Phys. Lett.* **2001**, *79*, 3164–3166. [[CrossRef](#)]
14. Khan, P.; Xu, Y.; Leond, W.; Adarsh, K.V.; Vezenov, D.; Biaggio, I.; Jain, H. Kinetics of photo-dissolution within Ag/As₂S₃ heterostructure. *J. Non-Cryst. Solids* **2018**, *500*, 468–474. [[CrossRef](#)]
15. Tanaka, K.; Sanjoh, H. Photodoping Dynamics in the Ag/As-S System. *J. Appl. Phys.* **1993**, *74*, 1106–1110. [[CrossRef](#)]
16. Gallais, L.; Bergeret, E.; Wang, B.; Guerin, M.; Bènevent, E. Ultrafast Laser Ablation of Metal Films on Flexible Substrates. *Appl. Phys. A* **2014**, *115*, 177–188. [[CrossRef](#)]
17. Angelov, I.B.; von Conta, A.; Trushin, S.A.; Major, Z.; Karsch, S.; Krausz, F.; Pervak, V. Investigation of the Laser-Induced Damage of Dispersive Coatings. In Proceedings of the Laser-Induced Damage in Optical Materials: 2011; SPIE: Bellingham, WA, USA, 2011; Volume 8190, pp. 117–123.

Disclaimer/Publisher’s Note: The statements, opinions and data contained in all publications are solely those of the individual author(s) and contributor(s) and not of MDPI and/or the editor(s). MDPI and/or the editor(s) disclaim responsibility for any injury to people or property resulting from any ideas, methods, instructions or products referred to in the content.